Dynamics of Atmospheres and Oceans 86 (2019) 1–9

Contents lists available at ScienceDirect

Dynamics of Atmospheres and Oceans

journal homepage: www.elsevier.com/locate/dynatmoce

The role of the Indian Ocean in determining the tropical pacific SST response to radiative forcing in an idealized model

Lei Zhang[a,*], De-Zheng Sun[a], Kristopher B. Karnauskas[a,b]

[a] Department of Atmospheric and Oceanic Sciences, University of Colorado, Boulder, CO, USA
[b] Cooperative Institute for Research in Environmental Sciences, University of Colorado, Boulder, CO, USA

ARTICLE INFO

Keywords:
Interbasin SST gradient
Radiative forcing
Global warming
Tropical Pacific response
Theoretical model

ABSTRACT

The complexity of the tropical climate system demands the development of a hierarchy of models to ensure our understanding of its response to anthropogenic forcing. The response of the tropical Pacific Ocean to radiative forcing has been studied previously with a box model. The model has provided insights into the tropical Pacific climate change that are otherwise not easily attainable. But that model only encompasses the tropical Pacific region. Recent studies have also shown that the Indian Ocean (IO) may be important in the response of the Pacific Walker circulation to radiative forcing, raising the need to expand the model to take into account the role of IO. This study presents the results concerning the tropical Pacific response to radiative forcing from an expanded-box model that includes the tropical IO, which influences the tropical Pacific through an inter-basin SST gradient.

The three-box model predicts an enhanced zonal SST gradient in tropical Pacific in response to the increased radiative forcing, similar to the previous two-box model. It is further noted that in the three-box model, a warmer IO relative to the Pacific enhances Pacific easterlies and subsequently strengthens the equatorial ocean circulation. Because of this ocean dynamical cooling, the warming response in the Pacific is effectively reduced in the three-box model that includes the role of IO compared with that in the two-box model. The role of the IO warming trend in enhancing the Pacific trade winds is confirmed using an atmospheric general circulation model experiment. These results may help to fully explain the relatively small observed warming trend in the tropical Pacific compared to that in the tropical IO evident in 20th century SST reconstructions.

1. Introduction

Changes in the tropical Pacific affect climate world-wide, as vividly evident in our rich experience with El Niño-Southern Oscillation (ENSO) (Hoskins and Karoly, 1981; Wallace and Gutzler, 1981; Jin, 1996; Wang et al., 2000; Xie et al., 2009). However, how the tropical Pacific changes in response to increase in the greenhouse effect remains uncertain (Knutson and Manabe, 1995; Vecchi et al., 2006; Vecchi and Soden, 2007; Tokinaga et al., 2012; Sandeep et al., 2014; Zhang and Li, 2014). The difficulty resides in the relatively short reliable observations for discerning the centennial-scale trend (DiNezio et al., 2013), and the substantial uncertainties in estimating the magnitude of the long-term sea surface temperature (SST) trend in the tropical Pacific between different SST reconstructions and climate model simulations (Vecchi and Soden, 2007; Karnauskas et al., 2009; Compo and Sardeshmukh,

* Corresponding author.
E-mail address: lezh8230@colorado.edu (L. Zhang).

https://doi.org/10.1016/j.dynatmoce.2019.02.003
Received 23 October 2018; Received in revised form 18 January 2019; Accepted 18 February 2019
Available online 21 February 2019
0377-0265/ © 2019 Elsevier B.V. All rights reserved.

2010; Sandeep et al., 2014; Zhang and Karnauskas, 2017).

Previous studies have postulated numerous theories for the response of the tropical Pacific SST to global warming. It has been suggested that the weakening of tropical Pacific zonal SST gradient in global climate models (GCMs) is attributable to the evaporative damping mechanism (Knutson and Manabe, 1995; Xie et al., 2010; Zhang and Li, 2014), the weakening of Walker circulation associated with atmospheric processes (Knutson and Manabe, 1995; Held and Soden, 2006; Vecchi and Soden, 2007; Zhang and Li, 2016) and the cloud feedback (Ramanathan and Collins, 1991; DiNezio et al., 2009).

Sun and Liu (1996) (SL96) explored the response of the tropical Pacific to the anthropogenic warming, using a simple two-box model. One important result from their box model analysis is that the zonal SST gradient may increase in response to an increase in the greenhouse effect, owing to the dynamical coupling between the atmosphere and ocean. Using the CZ model (Zebiak and Cane, 1987), a model with more complexity and has been used to successfully simulate some major aspects of ENSO, Clement et al. (1996) found similar results. These results emphasize the role of the oceanic upwelling that damps the initial SST warming in the eastern equatorial Pacific, which leads to stronger zonal SST gradients and hence strengthens easterly trade winds ("ocean dynamical thermostat mechanism"). Seager and Murtugudde (1997) found a qualitatively similar result (i.e., a strengthened zonal SST gradient) using a comprehensive oceanic general circulation model (OGCM), albeit with a weaker magnitude of the La Nina-like response due to the eventual warming of the upwelled water in the eastern tropical Pacific prior to subduction off the equator, and also possibly due to missing dynamical coupling.

On the other hand, it has been shown that a substantial warming trend emerges in the tropical Indian Ocean (IO) during the 20th century (Zhang, 2016; Zhang and Karnauskas, 2017; Zhang et al., 2018). Using atmospheric general circulation model (AGCM) experiments, recent studies have suggested that the Indian Ocean warming may play a role in forcing Walker circulation changes (Luo et al., 2012; Han et al., 2014; Zhang and Karnauskas, 2017). A recent study by Luo et al. (2017) has found that the underestimated interbasin warming contrast may contribute to the overestimated El Niño-like warming response under global warming in GCM projections. Given that it has been suggested that a hierarchy of models is needed for understanding the climate system (Held, 2005), and simple theoretical models have been shown to be a useful tool for understanding the tropical Pacific climate (SL96; Liang et al., 2012, 2017), it is useful to investigate the role of the Indian Ocean warming in the response of the tropical Pacific to the greenhouse effect in a simple model. However, both the box model of SL96 and the intermediate complexity model used by Clement et al. (1996) focus on the role of atmospheric, oceanic, or coupled processes *within* the tropical Pacific in determining the response of the Pacific coupled system to the greenhouse gas (GHG) forcing, and thus the role of the Indian Ocean has not been addressed. Here we consider the influence of the interbasin interaction on the tropical Pacific response to the GHG forcing in the theoretical framework as developed by SL96 but expanded to include the IO. We aim to shed further light on the relative insensitivity of tropical Pacific SST to the GHG forcing apparent in instrumental observations to date.

2. Models and data

2.1. Theoretical model

The two-box model in SL96 has been used to illustrate the importance of the local air-sea dynamic coupling to the formation of the tropical Pacific mean state, including a zonal SST gradient with a much lower mean SST in the eastern equatorial Pacific than would be expected based on a simple radiative-convective equilibrium. To examine the role of the interbasin interaction, we add a third box representing a tropical ocean basin adjacent to the western tropical Pacific, i.e., the tropical IO. The resulting model is employed in

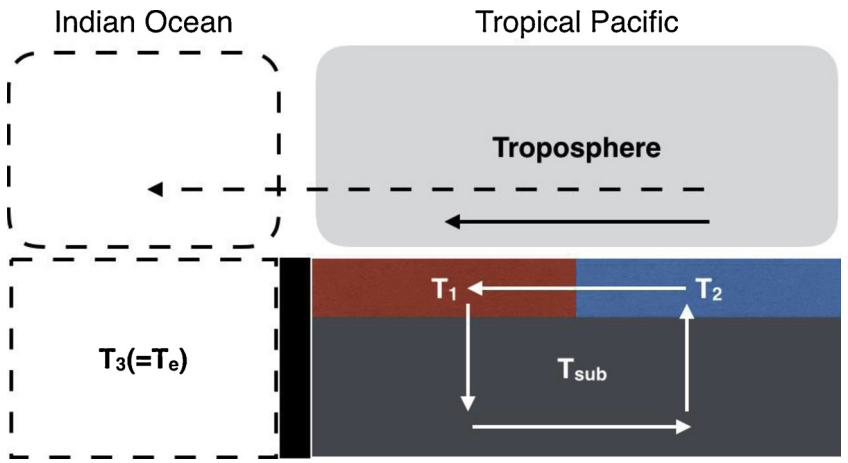

Fig. 1. A schematic diagram for the "three-box model" representing the air-sea coupled system encompassing both the tropical Pacific and the tropical Indian ocean. Shaded boxes represent the tropical Pacific Ocean, and dashed boxes for the tropical Indian Ocean. White arrows denote the ocean currents, and solid (dashed) black arrows represent the surface winds driven by the tropical Pacific zonal SST gradient (interbasin SST gradient).

this study and further elaborated upon below.

In the three-box model, T_1, T_2 and T_3 denote SST in the western and eastern tropical Pacific and the tropical IO, respectively (Fig. 1). T_e represents the radiative-convective equilibrium temperature, and T_{sub} for the subsurface ocean temperature in tropical Pacific. The tropical IO is assumed to be in a radiative-convective equilibrium state, with no interaction with the tropical Pacific; implication of this assumption is discussed in the summary section. Hence, T_1, T_2 and T_3 are controlled by the following equations:

$$\frac{\partial T_1}{\partial t} = c(T_e - T_1) + q(T_2 - T_1) \tag{1}$$

$$\frac{\partial T_2}{\partial t} = c(T_e - T_2) + q(T_{sub} - T_2) \tag{2}$$

$$\frac{\partial T_3}{\partial t} = c(T_e - T_3) \tag{3}$$

$$q = \alpha(T_1 - T_2) + \beta(T_3 - T_2) \tag{4}$$

where c denotes the reciprocal of the time scale for the thermodynamic damping process, and q represents oceanic dynamical processes, i.e., zonal advection in Eq. (1) and oceanic upwelling in Eq. (2). Naturally, the strength of q is proportional to the zonal SST gradients (T_1–T_2) and (T_3–T_2) by way of its coupling to the zonal wind stress along the equator (Eq. (4)). Note that the role of the interbasin SST gradient in Eq. (4) is consistent with recent studies that found easterly anomalies over the entire equatorial Pacific forced by the IO warming (Luo et al., 2012; Zhang and Karnauskas, 2017). Here we focus on the steady (equilibrium) state of the system described by these four equations, i.e., the time derivatives are equal to 0.

The main difference between this three-box model and that of SL96 lies in the formulation of q; the strength of ocean currents associated with coupling between the zonal SST gradient and the surface wind is now determined by two physical processes (Eq. (4)): *local air-sea coupling within the tropical Pacific region (α) and the remote impact of the tropical IO on Pacific low-level winds due to the interbasin SST gradient (β)* (Fig. 1). Note that $T_3 = T_e > T_2$ for the equilibrium state, which is consistent with higher SST in the Indian Ocean compared to the eastern equatorial Pacific in observations (Fig. 2). As a result, q is stronger in the three-box model compared to that in SL96 because of the interbasin interaction. Also note that the three-box model will be reduced to the two-box model in SL96 if one sets $\beta = 0$.

2.2. Atmospheric general circulation model

To confirm the role of the additional Indian Ocean warming trend in strengthening the Pacific easterly trades, numerical experiments using AGCM ECHAM4.6 (Roeckner et al., 1996) are performed. The model resolution is T42 with 19 vertical levels. In these experiments, monthly SST climatology is used to force the atmosphere globally, except for the tropical Indian Ocean where a 0.1 °C/decade SST warming trend is added. This SST warming rate is similar to the observed value (Fig. 2 and Table 1). An eight-member ensemble with slightly different initial conditions was obtained for analysis. For each ensemble member, the model was integrated for 40 years, and the first 5 years were discarded to allow the model to reach equilibrium.

2.3. Observational datasets

In this study, the instrumental SST reconstructions for the period 1900–2015 from the Hadley Centre Sea Ice and SST dataset

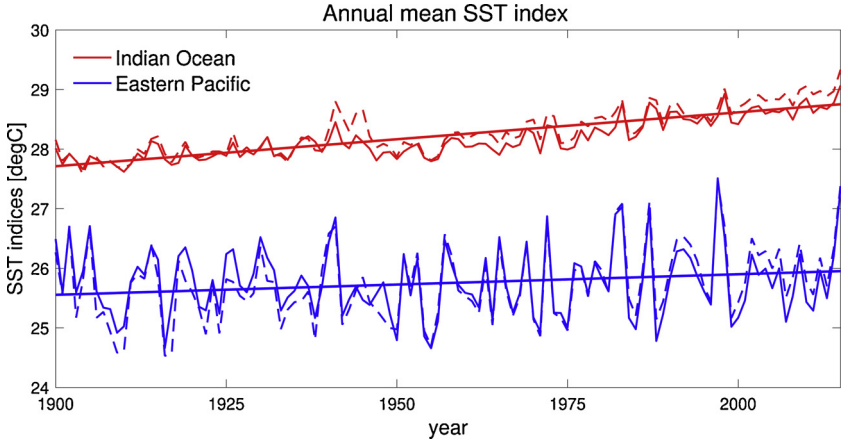

Fig. 2. Time series of annual mean SST averaged over the tropical Indian Ocean (red, 5 °N-5 °S, 40 °E-100 °E) and eastern tropical Pacific (blue, 5 °N-5 °S, 155 °W-80 °W). Unit is °C. Domains are marked in Fig. 6. Solid for HadISST and dashed for ERSSTv4 (For interpretation of the references to colour in this figure legend, the reader is referred to the web version of this article).

Table 1
Domain averaged SST warming trends during 1900–2015 in the three 20th century SST reconstructions. Units are K century^{-1}. Also shown in the table are the tropical Pacific SST warming trends relative to those in the tropical Indian Ocean. Domain 5 °N-5 °S, 40 °E-100 °E is chosen for the tropical Indian Ocean, 5 °N-5 °S, 130 °E-155 °W and 5 °N-5 °S, 155 °W-80 °W for the tropical western and eastern Pacific. Domains are marked in Fig. 6.

	IO	WP (WP/IO)	EP (EP/IO)
HadISST	0.83	0.33 (39%)	0.095 (11%)
ERSST	0.98	0.71 (72%)	0.60 (61%)
Kaplan	0.61	0.35 (57%)	0.13 (21%)

(HadISST; Rayner et al., 2003), the National Oceanic and Atmospheric Administration (NOAA) Extended Reconstructed SST dataset, version 4 (ERSSTv4; Huang et al., 2015) and the Kaplan SST dataset (Kaplan et al., 1998) are analyzed to explore the observed SST trend pattern. As shown below, the observed SST trend exhibits large warming in the IO, but negligible warming in the tropical Pacific. This inter-basin warming contrast motivates the experiment in this study, and we aim to use the three-box model to explain its physical causes. In this study, we did not analyze long-term changes of the Pacific Walker circulation using observational datasets, which are relatively uncertain and less reliable during the early 20th century (DiNezio et al., 2013).

3. Results

As demonstrated in SL96, the mean tropical Pacific SST is lower than predicted by a radiative-convective equilibrium state due to oceanic dynamical cooling processes in the box model ($T_1 < T_e$, $T_2 < T_e$) (Fig. 3a–c). Meanwhile, the air-sea dynamic coupling also gives rise to a zonal SST gradient in tropical Pacific (T_1–$T_2 > 0$). In addition, tropical Pacific SSTs (T_1 and T_2) increase in response to the GHG forcing in the box model, and so does the zonal SST 'gradient' (T_1–T_2), as found in SL96. Note that the enhanced radiative forcing associated with increases in GHG emission is represented by an increase in the radiative-convective equilibrium temperature T_e. The stronger tropical Pacific zonal SST gradient under global warming is consistent with the ocean dynamical thermostat mechanism, which emphasizes the oceanic dynamical cooling mechanism associated with the eastern Pacific upwelling (Clement et al., 1996; SL96).

In the two-box model (or in the present three-box model with $\beta = 0$), tropical Pacific SSTs are lower and become ~30% less sensitive to the GHG forcing when oceanic dynamical cooling processes are stronger, represented by a doubled air-sea coupling parameter α (Fig. 3d–f). This result confirms findings of SL96 and Clement et al. (1996) that stronger air-sea coupled dynamic processes within the equatorial Pacific may act against the radiative heating, leading to lower tropical Pacific SSTs. More importantly, we find that warming rates of T_1 and T_2 per degree increase in T_e are significantly reduced when the IO effect is included (i.e., where $\beta \neq 0$, Fig. 3g–i) compared to that in the two-box model (Fig. 3d–f). We set $\beta = \alpha/2$ in the three-box model because the distance between IO and the eastern Pacific is approximately twice as that between the western and the eastern Pacific (Fig. 1), and α is estimated based on observations (SL96). Therefore, air-sea coupling processes that involve the coupled zonal gradients of SST and sea level pressure and associated surface zonal wind and ocean currents would be around half magnitude of those associated with the local air-sea coupling in the tropical Pacific. Results are quantitatively similar with different β values, although a larger β reduces the Pacific warming response more significantly (Fig. 4). Also note that the tropical Pacific zonal SST 'gradient' (T_1–T_2) only increases slightly with increase in T_e in the three-box model, roughly one order of magnitude less than in the absence of the interbasin interaction (Fig. 3f and i). Similarly, increases in β leads to smaller changes in the zonal SST gradient in response to the GHG forcing (Fig. 4). Hence, it is clear that tropical Pacific SSTs become much less sensitive to the GHG forcing due to the IO impact in this simple theoretical framework. The IO effect also leads to a smaller T_1 as well as a weaker Pacific zonal SST gradient in the box model (Fig. 3f and i), despite stronger Pacific easterlies due to the interbasin SST gradient. The western Pacific cooling is due to the zonal SST advection anomaly associated with the enhanced westward ocean current as well as the T_2 cooling anomaly (Eq. (1)).

Why does the interbasin interaction limit the tropical Pacific SST warming response to GHG forcing in the real world? A higher IO SST compared to the eastern Pacific strengthens the tropical easterlies and accelerates the mean tropical Pacific currents (represented here as an increase in q) (Eq. (4)). As suggested in SL96, it is the competition between the radiative heating (determined by T_e) and the oceanic upwelling damping (influenced by T_{sub} and the parameter q) that determines the equilibrium SST in the tropical Pacific. Therefore, the stronger ocean dynamical damping due to the interbasin SST gradient imposes a stronger constraint on the tropical Pacific SST response to the increased radiative forcing.

Central to this mechanism is the assumption built in Eq. (4) that a positive SST anomaly in the tropical IO (relative to that in the eastern tropical Pacific) will result in easterly anomalies over the tropical Pacific. To further demonstrate the validity of this assumption, we have conducted AGCM experiments. In these experiments, we impose a 0.1 °C decade^{-1} SST warming trend in the tropical Indian ocean and examine responses in the tropical sea level pressure and surface winds. As shown in Fig. 5, the imposed warming trend in the SST over the tropical IO causes a local negative sea level pressure (SLP) trend, which extends to the western tropical Pacific as a Kelvin wave response, weakening the Pacific zonal SLP gradient. Consequently, low-level easterly anomalies appear over the tropical Pacific, strengthening the background easterlies (Fig. 5b). The enhanced Pacific trade winds would cause Pacific SST cooling anomalies through enhancing the equatorial upwelling and zonal temperature advection, and increasing the surface latent heat loss. In addition, although the strongest easterly wind and negative SLP anomalies induced by IO warming in

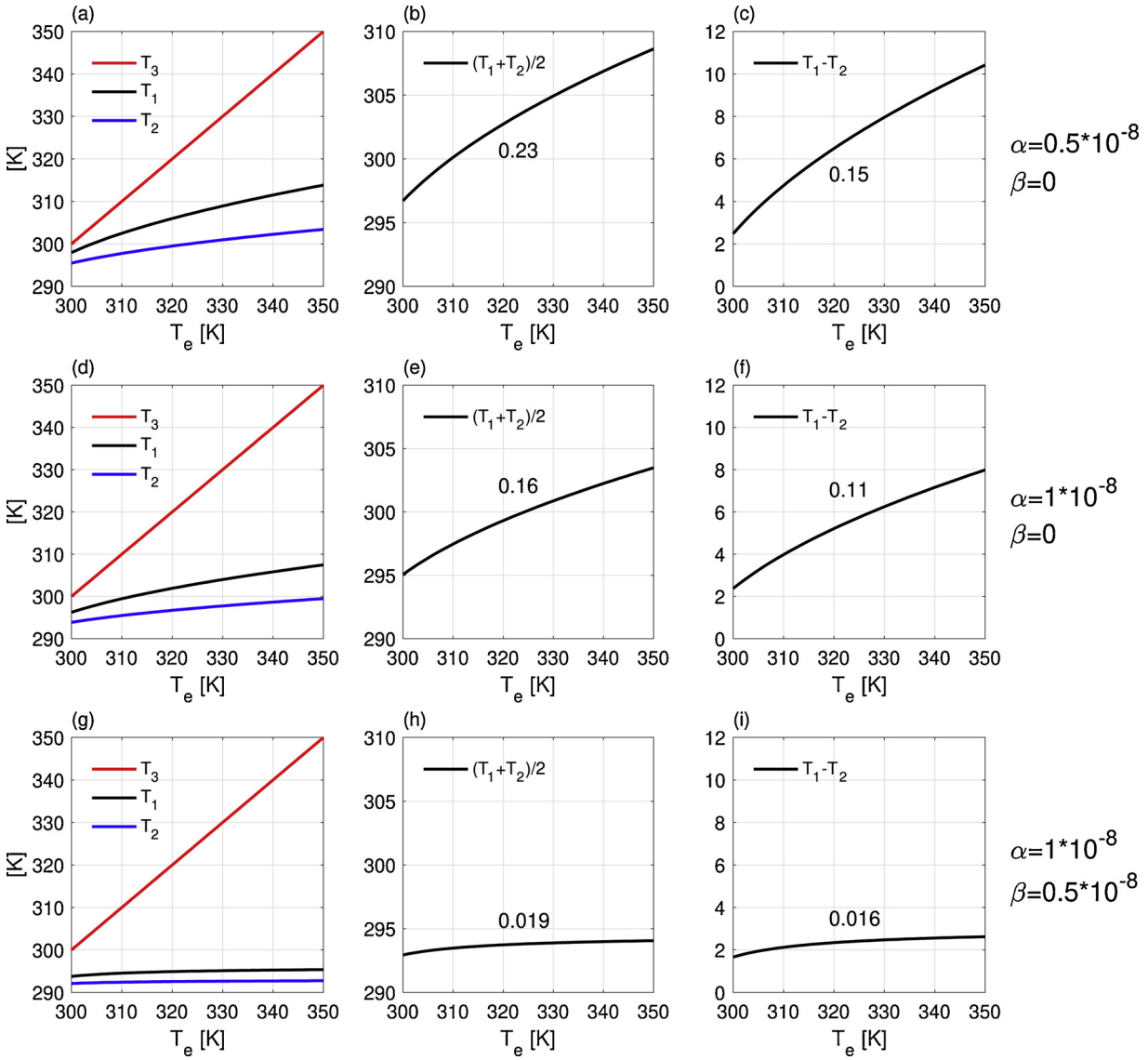

Fig. 3. Changes of T_1, T_2, T_3 (black, blue and red in the left column, respectively), $(T_1 + T_2)/2$ (mean tropical Pacific SST, middle column) and T_1–T_2 (tropical Pacific zonal SST gradient, right column) with increase in T_e. Unit is K. Numbers in the second and third columns denote slopes of the curves, i.e., changes per degree increase in T_e (T_3). Shown are results for different values of parameters α and β in the "three-box" model. Following SL96, we set α ~$1*10^{-8}$ K^{-1} s^{-1}, $c = 1.5*10^{-8}$ s^{-1} and $T_{sub} = 290$ K (For interpretation of the references to colour in this figure legend, the reader is referred to the web version of this article).

AGCM experiments are mostly located at the western tropical Pacific, those zonal wind anomalies could cause a sharper zonal thermocline slope in the equatorial Pacific, leading to thermocline shoaling and thus lower SST in the eastern tropical Pacific. Forcing an ocean model with the wind changes from this AGCM experiment is planned to quantify these expected oceanic responses.

4. Summary and discussion

Driven by the curiosity over the impact of climate change in the Indian ocean on the climate change in the tropical ocean, we have extended an influential box model for the tropical climate change (SL96) to include the tropical Indian ocean. The major difference between the current model and previous ones, e.g., the two-box model developed by SL96, lies in the addition of the tropical interbasin interaction. It is found that both the basin wide tropical Pacific SST and its zonal SST gradient increase in response to the increased radiative forcing, which is consistent with findings of SL96 and others. More importantly, the warming rate of tropical Pacific in response to the GHG forcing is significantly reduced compared to the two-box model, which is associated with the more active oceanic dynamical cooling processes in the tropical Pacific driven by the enhanced tropical Pacific easterlies due to inclusion of the IO and the associated interbasin SST gradient. The hypothesized role of IO warming trend in strengthening the Pacific easterlies is

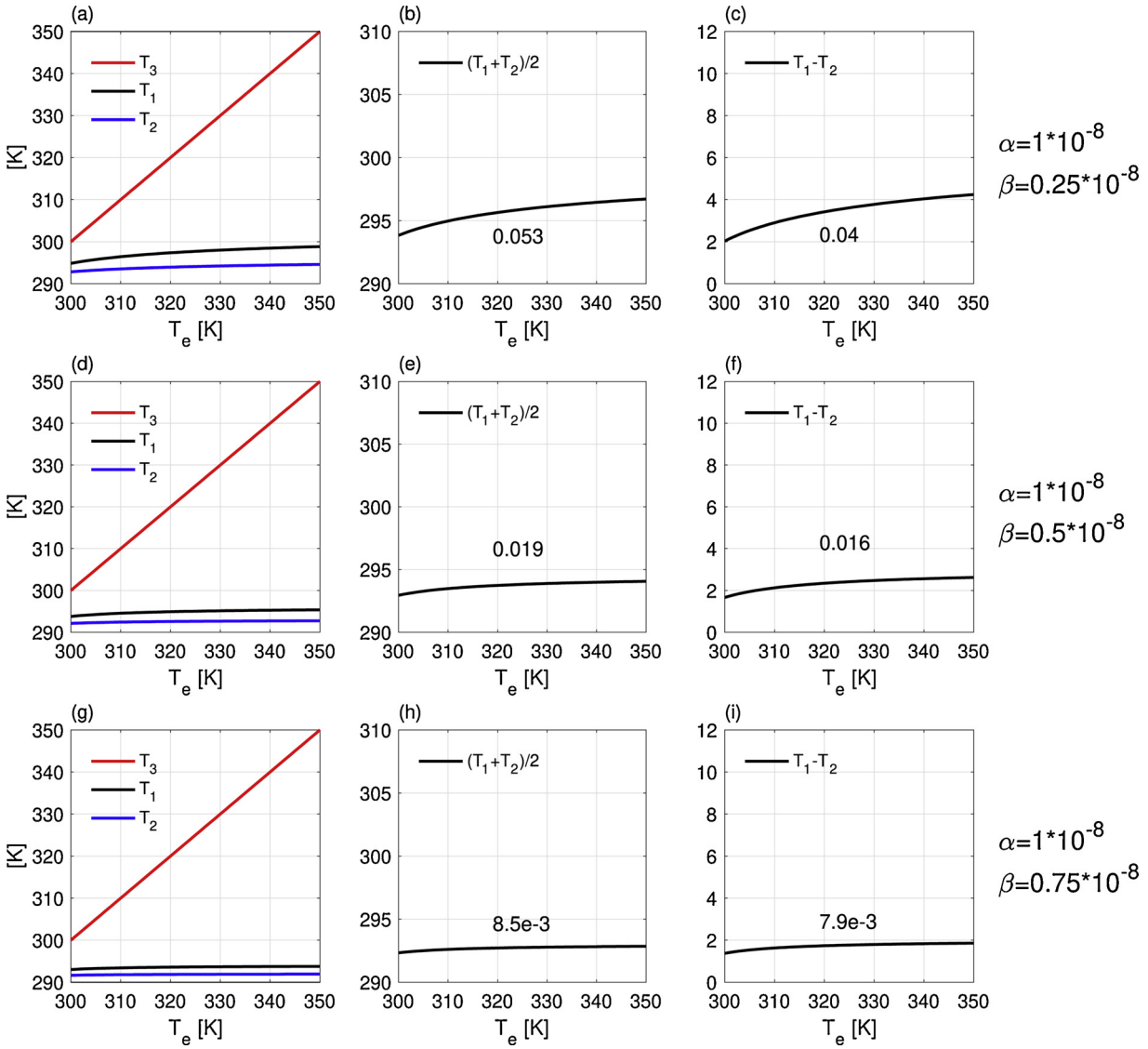

Fig. 4. Same as Fig. 3, but for different values of α and β.

confirmed using AGCM experiments.

The tropical Pacific SST and its zonal SST gradient has been only slightly enhanced or exhibits a negligible trend compared to the tropical IO, according to 20th century SST reconstructions (Fig. 6 and Table 1). It is also noted that there are relatively large discrepancies in the SST trend pattern among different SST reconstructions, with small eastern Pacific cooling in HadISST and Kaplan SST, and warming in ERSSTv4. These discrepancies could be due to sparse observations during the early 20th century (Deser et al., 2010) and/or different estimates of ENSO signals in these reconstructions (Solomon and Newman, 2012). Nevertheless, the observed SST trend pattern is distinctly different from the predicted El-Niño like SST response in GCMs (Held and Soden, 2006; Vecchi and Soden, 2007; Coats and Karnauskas, 2017), but is in qualitative agreement with the ocean thermostat mechanism predicted by CZ-type models and uncoupled OGCMs, i.e. a La Niña-like SST trend. Regardless of the sign, the observed magnitude of the tropical Pacific SST response to radiative forcing is much weaker than that predicted by either type of model or theory, while it is to some extent consistent with the negligible tropical Pacific warming response due to the interbasin SST gradient in the three-box model. Given the evident differences between observed and simulated Pacific SST warming trend and the prominent role of the IO warming in determining the Pacific SST warming response, it is important to analyze whether the CMIP5 models can faithfully capture the IO warming impact on the Pacific SST changes. It has also been noted that the poor simulation of ENSO asymmetry and relatedly the lack of or weaker time-mean effect of ENSO in the CMIP5 models may also be important in explaining the different long-term SST trend pattern between observations and CMIP5 models (Zhang and Sun, 2014; Sun et al., 2014; Ogata et al., 2013). Exploring the causes of the model/data discrepancies is important for future climate prediction and demands further attention.

Note that the warming rate of the IO SST is greater than that in the tropical Pacific in both observations and the three-box model

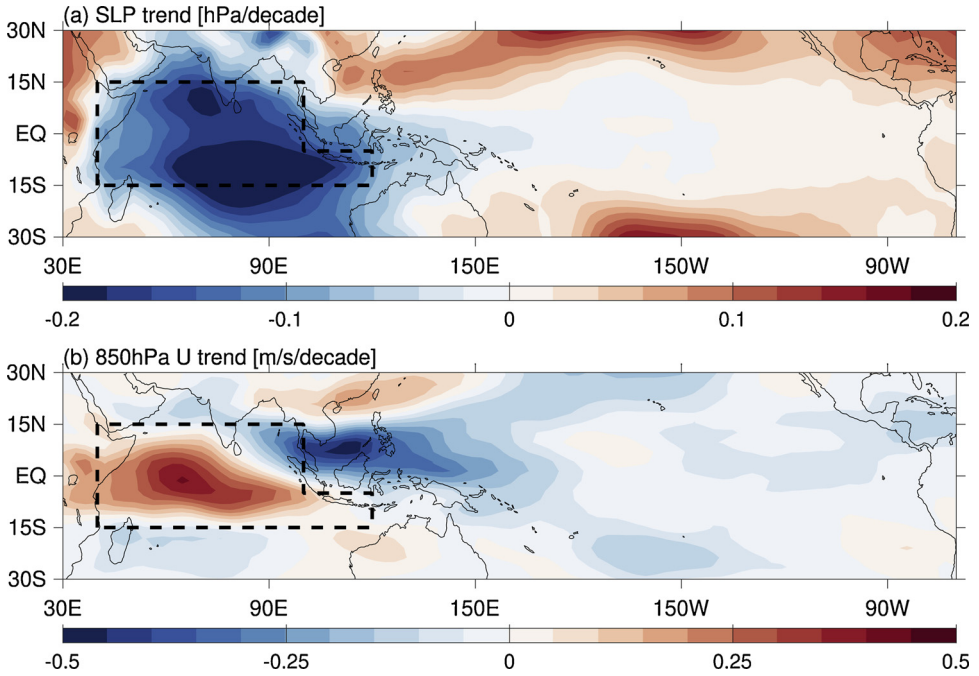

Fig. 5. (a) SLP trends in the tropical Indo-Pacific region in response to a prescribed warming trend (0.1 °C decade^{-1}) in the tropical Indian ocean, simulated by the AGCM experiments. Units are hPa decade^{-1}. (b) Same as (a) but for the trend of 850 hPa zonal wind (m s^{-1} decade^{-1}). Shown are the average of the results from the eight-member ensemble. The region where the 0.1 °C decade^{-1} SST warming trend is added is marked by the black dashed line.

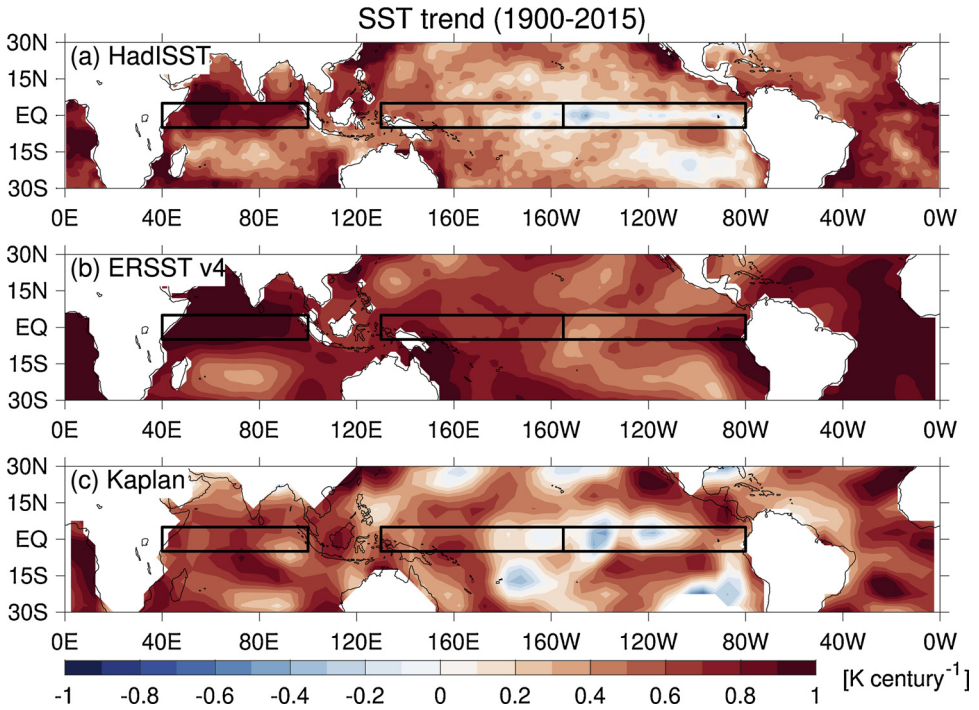

Fig. 6. Linear trend of SST during 1900-2015 for (a) HadISST (b) ERSST v4 and (c) Kaplan SST datasets. Units are K century^{-1}.

(Figs. 3 and 6 and Table 1). Under global warming, tropical SSTs rise in response to the GHG forcing. However, unlike the tropical IO, surface warming in the eastern equatorial Pacific is limited initially by the oceanic dynamical cooling associated with the strong mean-state upwelling and the enhanced stratification. Such a differential warming pattern leads to an enhanced interbasin SST

gradient, which further strengthens the coupled dynamical cooling process in tropical Pacific in a warmer climate. This process may subsequently limit the tropical Pacific SST warming response and thus further enhances the interbasin SST gradient.

It is also interesting to assume a smaller warming rate in the IO compared to the tropical Pacific in response to the GHG forcing. In this case, one would expect decreasing interbasin SST gradient under global warming and as a result, an increasing warming rate in the tropical Pacific with increase in T_e. Eventually, the interbasin SST gradient between the tropical IO and the eastern Pacific would become negligible and the sensitivity of tropical Pacific SSTs to the GHG forcing would be the same as that in the two-box model. This illustrates the importance of the ocean dynamical thermostat mechanism that initially limits the eastern Pacific warming and thus enhances the interbasin SST gradient. Otherwise, the role of the interbasin interaction in tropical Pacific response would be weakened.

Results presented in this study do not conflict with previous ones that successfully simulate climate mean state and/or ENSO using the two-box model or similar intermediate complexity models. In previous studies, the primary goal was to analyze the natural variability of the tropical Pacific, in which the local air-sea coupling in the tropical Pacific plays a dominant role, whereas the tropical IO/Atlantic Ocean plays a passive and delayed role, responding to changes in the tropical Pacific. For example, on interannual timescales, the tropical IO SST variability is predominantly controlled by the tropical Pacific forcing, i.e., ENSO (Klein et al., 1999; Alexander et al., 2002). The dynamics governing the response to the external forcing, however, differs substantially from the natural variability of the climate system on a particular time-scale, as evident in analysis of more comprehensive models (DiNezio et al., 2011). Hence, the inter-basin processes that play the leading role can be different on different timescales.

In this study, the tropical IO is assumed to be in radiative-convective equilibrium, while the physical processes that may affect the tropical IO SST, including remote impact of the Pacific Walker circulation changes and changes of the Indonesian Throughflow, are not included in the simple three-box model. Moreover, it has been shown that the Atlantic can drive Pacific variability at multi-decadal timescales (Kucharski et al., 2015; Sun et al., 2017), and the tropical Atlantic SST warming can induce a strengthened Walker circulation (McGregor et al., 2014; Li et al., 2016; Zhang and Karnauskas, 2017), whereas we only consider the impact of tropical IO in this study. A future adaptation of the present theoretical model to analyze the impact of these physical processes on the tropical Pacific is warranted. Note that the present simple theoretical model is meant to be a first step for understanding results from more complicated climate models, following the suggestion from Held (2005) that developing a hierarchy of models may be a necessary strategy in understanding our climate. Indeed, the recent study by Liang et al. (2012, 2017) has provided an illuminating example how a box model can simulate a crucial aspect of ENSO while most of the state-of-the-art models cannot. The complementary nature of the simple models to the more complex global climate models should be more fully exploited.

Acknowledgement

NOAA ERSSTv4 data and Kaplan SST v2 are provided by the NOAA/OAR/ESRL PSD, Boulder, Colorado, USA, from their web site at http://www.esrl.noaa.gov/psd/. HadISST dataset is available at http://www.metoffice.gov.uk/hadobs/hadisst/.

References

Alexander, M.A., Bladé, I., Newman, M., Lanzante, J.R., Lau, N.-C., Scott, J.D., 2002. The atmospheric bridge: the influence of ENSO teleconnections on air–sea interaction over the global oceans. J. Clim. 15, 2205–2231. https://doi.org/10.1175/1520-0442(2002)015<2205:TABTIO>2.0.CO;2.

Clement, A.C., Seager, R., Cane, M.A., Zebiak, S.E., 1996. An ocean dynamical thermostat. J. Clim. 9, 2190–2196. https://doi.org/10.1175/1520-0442(1996)009<2190:AODT>2.0.CO;2.

Coats, S., Karnauskas, K.B., 2017. Are simulated and observed 20th century tropical Pacific sea surface temperature trends significant relative to internal variability? Geophys. Res. Lett. 44, 9928–9937. https://doi.org/10.1002/2017GL074622.

Compo, G.P., Sardeshmukh, P.D., 2010. Removing ENSO-Related variations from the climate record. J. Clim. 23, 1957–1978. https://doi.org/10.1175/2009JCLI2735.1.

Deser, C., Phillips, A.S., Alexander, M.A., 2010. Twentieth century tropical sea surface temperature trends revisited. Geophys. Res. Lett. 37. https://doi.org/10.1029/2010GL043321.

DiNezio, P.N., Clement, A.C., Vecchi, G.A., Soden, B.J., Kirtman, B.P., Lee, S.-K., 2009. Climate response of the equatorial pacific to global warming. J. Clim. 22, 4873–4892. https://doi.org/10.1175/2009JCLI2982.1.

DiNezio, P., Clement, A., Vecchi, G., 2011. Reconciling differing views of tropical Pacific climate change. Eos Trans. Am. Geophys. Union 91, 141–142. https://doi.org/10.1029/2010EO160001.

DiNezio, P.N., Vecchi, G.A., Clement, A.C., 2013. Detectability of changes in the walker circulation in response to global warming*. J. Clim. 26, 4038–4048. https://doi.org/10.1175/JCLI-D-12-00531.1.

Han, W., Coauthors, 2014. Intensification of decadal and multi-decadal sea level variability in the western tropical Pacific during recent decades. Clim. Dyn. 43, 1357–1379. https://doi.org/10.1007/s00382-013-1951-1.

Held, I.M., 2005. The gap between simulation and understanding in climate modeling. Bull. Am. Meteorol. Soc. 86, 1609–1614. https://doi.org/10.1175/BAMS-86-11-1609.

Held, I.M., Soden, B.J., 2006. Robust responses of the hydrological cycle to global warming. Bull. Am. Meteorol. Soc. 19, 5686–5699. https://doi.org/10.1175/JCLI3990.1.

Hoskins, B.J., Karoly, D.J., 1981. The steady linear response of a spherical atmosphere to thermal and orographic forcing. J. Atmos. Sci 38, 1179–1196. https://doi.org/10.1175/1520-0469(1981)038<1179:TSLROA>2.0.CO;2.

Huang, B., Coauthors, 2015. Extended reconstructed sea surface temperature version 4 (ERSST.v4). Part I: upgrades and intercomparisons. J. Clim. 28, 911–930. https://doi.org/10.1175/JCLI-D-14-00006.1.

Jin, F.F., 1996. Tropical ocean-atmosphere interaction, the pacific cold tongue, and the el nino-southern oscillation. Science 274, 76–78. https://doi.org/10.1126/science.274.5284.76.

Kaplan, A., Cane, M.A., Kushnir, Y., Clement, A.C., Blumenthal, M.B., Rajagopalan, B., 1998. Analyses of global sea surface temperature 1856–1991. J. Geophys. Res. Oceans 103, 18567–18589. https://doi.org/10.1029/97JC01736.

Karnauskas, K.B., Seager, R., Kaplan, A., Kushnir, Y., Cane, M.A., 2009. Observed strengthening of the zonal sea surface temperature gradient across the Equatorial Pacific Ocean*. J. Clim. 22, 4316–4321. https://doi.org/10.1175/2009JCLI2936.1.

Klein, S.A., Soden, B.J., Lau, N.-C., 1999. Remote sea surface temperature variations during ENSO: evidence for a tropical atmospheric bridge. J. Clim. 12, 917–932. https://doi.org/10.1175/1520-0442(1999)012<0917:RSSTVD>2.0.CO;2.
Knutson, T.R., Manabe, S., 1995. Time-mean response over the tropical pacific to increased CO2 in a coupled ocean-atmosphere model. J. Clim. 8, 2181–2199. https://doi.org/10.1175/1520-0442(1995)008<2181:TMROTT>2.0.CO;2.
Kucharski, F., Coauthors, 2015. Atlantic forcing of Pacific decadal variability. Clim. Dyn. 46, 2337–2351. https://doi.org/10.1007/s00382-015-2705-z.
Li, X., Xie, S.-P., Gille, S.T., Yoo, C., 2016. Atlantic-induced pan-tropical climate change over the past three decades. Nat. Clim. Change 6, 275–279. https://doi.org/10.1038/nclimate2840.
Liang, J., Yang, X.-Q., Sun, D.-Z., 2012. The effect of ENSO events on the tropical pacific mean climate: insights from an analytical model. J. Clim. 25, 7590–7606. https://doi.org/10.1175/JCLI-D-11-00490.1.
Liang, J., Yang, X.-Q., Sun, D.-Z., 2017. Factors determining the asymmetry of ENSO. J. Clim. 30, 6097–6106. https://doi.org/10.1175/JCLI-D-16-0923.1.
Luo, J.-J., Sasaki, W., Masumoto, Y., 2012. Indian Ocean warming modulates Pacific climate change. Proc. Natl. Acad. Sci. U. S. A. 109, 18701–18706. https://doi.org/10.1073/pnas.1210239109.
Luo, J.-J., Wang, G., Dommenget, D., 2017. May common model biases reduce CMIP5's ability to simulate the recent Pacific La Niña-like cooling? Clim. Dyn. 112, C11007–C11017. https://doi.org/10.1007/s00382-017-3688-8.
McGregor, S., Timmermann, A., Stuecker, M.F., England, M.H., Merrifield, M., Jin, F.-F., Chikamoto, Y., 2014. Recent Walker circulation strengthening and Pacific cooling amplified by Atlantic warming. Nat. Clim. Change 4, 888–892. https://doi.org/10.1038/nclimate2330.
Ogata, T., Xie, S.-P., Wittenberg, A., Sun, D.-Z., 2013. Interdecadal amplitude modulation of El Nino/Southern Oscillation and its impacts on tropical Pacific decadal variability. J. Clim. 26, 7280–7297.
Ramanathan, V., Collins, W., 1991. Thermodynamic regulation of ocean warming by cirrus clouds deduced from observations. Nature 351, 27–32.
Rayner, N.A., Parker, D.E., Horton, E.B., Folland, C.K., Alexander, L.V., Rowell, D.P., Kent, E.C., Kaplan, A., 2003. Global analyses of sea surface temperature, sea ice, and night marine air temperature since the late nineteenth century. J. Geophys. Res. 108, 4407. https://doi.org/10.1029/2002JD002670.
Roeckner, E., Coauthors, 1996. The atmospheric general circulation model ECHAM-4: model description and simulation of present-day climate. Clim. Dyn. 218.
Sandeep, S., Stordal, F., Sardeshmukh, P.D., Compo, G.P., 2014. Pacific Walker Circulation variability in coupled and uncoupled climate models. Clim. Dyn. 43, 103–117. https://doi.org/10.1007/s00382-014-2135-3.
Seager, R., Murtugudde, R., 1997. Ocean dynamics, thermocline adjustment, and regulation of tropical SST. J. Clim. 10, 521–534. https://doi.org/10.1175/1520-0442(1997)010<0521:ODTAAR>2.0.CO;2.
Solomon, A., Newman, M., 2012. Reconciling disparate twentieth-century Indo-Pacific ocean temperature trends in the instrumental record. Nat. Clim. Change 2, 691–699. https://doi.org/10.1038/nclimate1591.
Sun, D.-Z., Liu, Z., 1996. Dynamic ocean-atmosphere coupling: a thermostat for the tropics. Science 272, 1148–1150.
Sun, D.-Z., Zhang, T., Sun, Y., Yu, Y., 2014. Rectification of El Nino-Southern Oscillation into Climate Anomalies of Decadal and Longer Time-scales: Results from Forced Ocean GCM Experiments. J. Clim. 27, 2545–2561.
Sun, C., Kucharski, F., Li, J., Jin, F.-F., Kang, I.-S., Ding, R., 2017. Western tropical Pacific multidecadal variability forced by the Atlantic multidecadal oscillation. Nat. Commun. 8, 15998. https://doi.org/10.1038/ncomms15998.
Tokinaga, H., Xie, S.-P., Deser, C., Kosaka, Y., Okumura, Y.M., 2012. Slowdown of the Walker circulation driven by tropical Indo-Pacific warming. Nature 491, 439–443. https://doi.org/10.1038/nature11576.
Vecchi, G.A., Soden, B.J., 2007. Global warming and the weakening of the tropical circulation. J. Clim. 20, 4316–4340. https://doi.org/10.1175/JCLI4258.1.
Vecchi, G.A., Soden, B.J., Wittenberg, A.T., Held, I.M., Leetmaa, A., Harrison, M.J., 2006. Weakening of tropical Pacific atmospheric circulation due to anthropogenic forcing. Nature 441, 73–76. https://doi.org/10.1038/nature04744.
Wallace, J.M., Gutzler, D.S., 1981. Teleconnections in the geopotential height field during the Northern Hemisphere Winter. Mon. Weather. Rev 109, 784–812. https://doi.org/10.1175/1520-0493(1981)109<0784:TITGHF>2.0.CO;2.
Wang, B., Wu, R., Fu, X., 2000. Pacific–East Asian Teleconnection: How Does ENSO Affect East Asian Climate? J. Clim. 13, 1517–1536. https://doi.org/10.1175/1520-0442(2000)013<1517:PEATHD>2.0.CO;2.
Xie, S.-P., Hu, K., Hafner, J., Tokinaga, H., Du, Y., Huang, G., Sampe, T., 2009. Indian ocean capacitor effect on indo–western pacific climate during the summer following el niño. J. Clim. 22, 730–747. https://doi.org/10.1175/2008JCLI2544.1.
Xie, S.-P., Deser, C., Vecchi, G.A., Ma, J., Teng, H., Wittenberg, A.T., 2010. Global warming pattern formation: sea surface temperature and rainfall*. J. Clim. 23, 966–986. https://doi.org/10.1175/2009JCLI3329.1.
Zebiak, S.E., Cane, M.A., 1987. A model el niño–Southern oscillation. Mon. Weather Rev 115, 2262–2278. https://doi.org/10.1175/1520-0493(1987)115<2262:AMENO>2.0.CO;2.
Zhang, L., 2016. The roles of external forcing and natural variability in global warming hiatuses. Clim. Dyn. 47, 3157–3169. https://doi.org/10.1007/s00382-016-3018-6.
Zhang, L., Karnauskas, K.B., 2017. The Role of Tropical Interbasin SST Gradients in Forcing Walker Circulation Trends. J. Clim. 30, 499–508. https://doi.org/10.1175/JCLI-D-16-0349.1.
Zhang, L., Li, T., 2014. A simple analytical model for understanding the formation of sea surface temperature patterns under global warming. J. Clim. 27, 8413–8421. https://doi.org/10.1175/JCLI-D-14-00346.1.
Zhang, L., Li, T., 2016. Relative roles of differential SST warming, uniform SST warming and land surface warming in determining the Walker circulation changes under global warming. Clim. Dyn. 48, 987–997. https://doi.org/10.1007/s00382-016-3123-6.
Zhang, T., Sun, D.-Z., 2014. ENSO Asymmetry in CMIP5 models. J. Clim. 27, 4070–4093.
Zhang, L., Han, W., Sienz, F., 2018. Unraveling causes for the changing behavior of tropical Indian Ocean in the past few decades. J. Clim. 31 (6), 2377–2388. https://doi.org/10.1175/JCLI-D-17-0445.1.